Biochimica et Biophysica Acta 1807 (2011) 80–84

Contents lists available at ScienceDirect

Biochimica et Biophysica Acta

journal homepage: www.elsevier.com/locate/bbabio

The identity of the transient proton loading site of the proton-pumping mechanism of cytochrome *c* oxidase ☆

Ville R.I. Kaila [a,b,*,1], Vivek Sharma [a], Mårten Wikström [a,*]

[a] Helsinki Bioenergetics Group, Programme of Structural Biology and Biophysics, Institute of Biotechnology, University of Helsinki, P.O. Box 65, FI-00014 Helsinki, Finland
[b] Department of Chemistry, University of Helsinki, P.O. Box 55, FI-00014 Helsinki, Finland

ARTICLE INFO

Article history:
Received 29 June 2010
Received in revised form 26 August 2010
Accepted 31 August 2010
Available online 8 September 2010

Keywords:
Proton pump
Heme-copper oxidase
MD simulation
Proton-coupled electron transfer
Continuum electrostatics

ABSTRACT

Cellular respiration is driven by cytochrome *c* oxidase (C*c*O), which reduces oxygen to water and couples the released energy to proton pumping across the mitochondrial or bacterial membrane. Proton pumping in C*c*O involves proton transfer from the negatively charged side of the membrane to a transient proton-loading or pump site (PLS), before it is ejected to the opposite side. Although many details of the reaction mechanism are known, the exact location of the PLS has remained elusive. We report here results from combined classical molecular dynamics simulations and continuum electrostatic calculations, which show that the hydrogen-bonded system around the A-propionate of heme a_3 dissociates reversibly upon reduction of heme *a*. The dissociation increases the pK_a value of the propionate to a value above ~9, making it accessible for redox-state dependent protonation. The redox state of heme *a* is of key importance in controlling proton leaks by polarizing the PLS both statically and dynamically. These findings suggest that the propionate region of heme a_3 fulfills the criteria of the pump site in the proton translocation mechanism of C*c*O.

1. Introduction

Cytochrome *c* oxidase (C*c*O) uses the energy released by oxygen reduction to pump protons across the mitochondrial or bacterial membrane [1–3]. Establishment of an electrochemical proton gradient or *protonmotive force* across the membrane is the key step in primary biological energy transduction. The proton gradient is further employed for synthesis of ATP by F_0F_1-ATPase and for active transport [4,5].

For catalyzing oxygen reduction, C*c*O receives stepwise four electrons from the soluble electron carrier protein cytochrome *c* (cyt *c*) at the positively charged side of the membrane (P-side). Electron transfer from cyt *c* to molecular oxygen takes place through the metal centers of C*c*O: Cu_A, heme *a* and the heme a_3/Cu_B binuclear center (BNC) (Fig. 1). Electron transfer in C*c*O is tightly coupled to proton transfer [1,6,7]. The protons are taken up from the negatively charged side of the membrane (N-side) (Fig. 1). In contrast to electron transfer, where tunneling can take place also at long donor–acceptor distances, protons are conducted through specific proton "channels" [8–10]. C*c*O employs two such channels; the D-channel named after a conserved Asp-91, and the K-channel, named after Lys-319 (Fig. 1). All pumped protons are transferred via the former, whereas two of the four protons required for oxygen reduction chemistry are transferred through the K-channel [11].

The D-channel ends at a conserved residue, Glu-242, in the middle of the membrane. Upon reduction of heme *a*, a proton is transferred, through the assistance of water molecules, from this residue to a proton-loading site (PLS) or "pump-site", which is known from electrometric measurements to be located approximately 1/5 of the dielectric thickness of the membrane from the P-side [6]. Analysis of these experiments suggested that the propionate group of heme a_3, or its immediate surroundings, may be identified as a likely proton-loading site [7,12,13]. Protonation of the PLS increases the midpoint potential of heme a_3, which leads to electron transfer from heme *a* to the BNC followed by proton transfer from Glu-242 to this site to form the equivalent of water [6]. The annihilation of the electron charge by the proton leads to the release of the proton from the PLS to the P-side of the membrane. At this stage of the reaction sequence there is a great risk for the proton to leak backwards to Glu-242, instead of being ejected to the P-side. It has been suggested that both kinetic and thermodynamic asymmetry in the position of the Glu-242 side chain might play an important role in preventing such a leak [14].

The propionate region of heme a_3 has been previously suggested to be a possible candidate for a pump-site [7,15–18]. Wikström et al. [15] found that the strong ion-pair between Arg-438 and the D-propionate

Abbreviations: C*c*O, Cytochrome *c* Oxidase; BNC, Binuclear Center; Glu, Glutamic Acid; Asp, Aspartic Acid; MD, Molecular Dynamics; PLS, Proton-loading Site

☆ Amino acid numbering corresponds to aa_3-type cytochrome *c* oxidase from *Bos taurus*.

* Corresponding authors. Helsinki Bioenergetics Group, Programme of Structural Biology and Biophysics, Institute of Biotechnology, University of Helsinki, P.O. Box 65, FI-00014 Helsinki, Finland. Tel.: +358 9 191 58000; fax: +358 9 191 59920.
E-mail addresses: ville.kaila@nih.gov (V.R.I. Kaila), marten.wikstrom@helsinki.fi (M. Wikström).
[1] Present address: Laboratory of Chemical Physics, National Institutes of Diabetes and Kidney and Digestive Diseases, National Institutes of Health, Bethesda, MD 20892-0520, USA.

0005-2728/$ – see front matter © 2010 Elsevier B.V. All rights reserved.
doi:10.1016/j.bbabio.2010.08.014

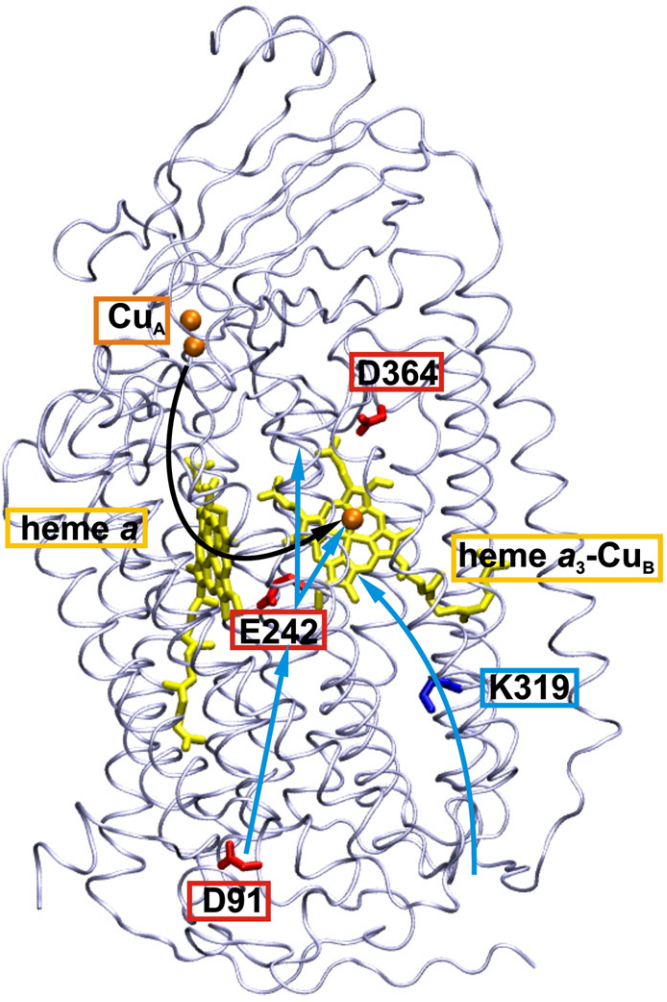

Fig. 1. The structure of CcO from *B. taurus* (PDB entry 1V54 [32]). Proton pathways are shown with blue arrows, electron transfer path with black arrow. Functionally critical acidic (red boxes) and basic (blue box) amino acid residues are highlighted, along with metal centers (orange and yellow boxes). The figure was prepared using VMD [44].

of heme a_3 may dissociate upon reduction of heme *a*. Empirical valence bond (EVB) studies [17,18] have also indicated that reduction of heme *a* might assist in proton transfer from Glu-242 to the D-propionate of heme a_3. However, thus far continuum electrostatic calculations by several groups have failed to find that this site would be in a pK range accessible for protonation [19–26]. Recently, Lee et al. [27] suggested that the D-propionate of heme a_3 is itself an unlikely pump site since certain mutations of Arg-438, which is the hydrogen bonding partner of the D-propionate, did not affect the pumping efficiency.

Quantum chemical calculations by Siegbahn et al. [16] showed that the pK_a-value of the A-propionate of heme a_3 increases upon reduction of the BNC. According to present mechanistic understanding [6,7,12,28,29], protonation of the PLS should take place prior to reduction of the BNC. It has also been suggested that His-291, which is a part of the BNC, might undergo large redox state dependent pK_a shifts [20–22]. However, detailed electrostatic studies by Fadda et al. [23,24] and Song et al. [25,26] did not find support for this hypothesis. Incorporation of the Glu-valve mechanism [14,28] further supported the notion that the A-propionate of heme a_3 might work as the pump site in CcO. Based on master equation approaches, Kim et al. [30,31] found that a pump-site that electrostatically couples to the redox-state of the metal centers increases the efficiency of the pumping machinery.

To gain insight in the molecular location of the PLS, we present results on full atomistic molecular dynamics (MD) simulations combined with continuum electrostatics. We observed that the A-propionate group of heme a_3 undergoes a transient and reversible conformational change that dissociates H-bonding from a nearby aspartic acid, and which increases its pK_a making it accessible for protonation.

2. Methods

2.1. Classical molecular dynamics simulations

The computational model system was built from PDB entry 1V54 of cytochrome *c* oxidase subunits I and II from *Bos taurus* [32]. Standard CHARMM27 [33] force field parameters were used for amino acids, and the metal centers were described by our in-house parameterization, which is based on large scale high-level quantum chemical calculations [34]. As suggested by PMF calculations [35], four water molecules were included in the non-polar cavity above Glu-242, which was modeled in its protonated form. MD simulations were performed with MD-package NAMD2 [36], controlling the temperature at $T = 310$ K with Langevin dynamics, and using a electrostatic cutoff of 20 Å, and an integration time step of 1 fs. CcO was simulated in three different redox states which are denoted as ox/ox, red/ox and ox/red, in which the former describes the redox state of heme *a* (oxidized or reduced). The latter describes the redox state of the binuclear site; in both states heme a_3 is in its ferryl form (heme a_3[IV] = O^{2-}) and Cu_B is cupric with a hydroxide as the fourth ligand. "ox" denotes the so-called $\mathbf{P_M}$ state where the covalently bonded Tyr-244 is in the neutral radical form while "red" denotes state $\mathbf{P_R}$ with Tyr-244 as the anionic tyrosinate. All amino acids were in their standard protonation states, except Glu-242 and Asp-364, which were in their protonated forms. As His-368 is ligated to the magnesium atom above the heme a_3 propionates, it is most probably singly protonated. Preliminary test calculation also suggested that Asp-364 prefers protonation over the A-propionate, in agreement with previous electrostatic calculations [19] and quantum chemical optimizations [34], both suggesting that the proton stays coordinated with the Asp. Simulations on the three redox-states were carried out for 5 ns, after initial minimization and equilibration.

2.2. Continuum electrostatic calculations

Representative structures of *open* and *closed* (see Section 3) conformations of the PLS obtained from MD simulations were used to calculate the pK_a-values with continuum electrostatics calculations. Average pK_a-values of the PLS in the respective redox states were also calculated from a set of nine different structures representing the "open" conformation, chosen based on the Asp-364 hydroxyl (atom HD2)/heme a_3 A-propionate (atom O1A) distance larger than 4.5 Å, and the A-propionate twisting dihedral angle (atoms CAA-CBA-CGA-O1A) smaller than 20°. The continuum electrostatic calculations were done with the MULTIFLEX module in program package MEAD [37,38], which is a numerical Poisson–Boltzmann equation solver based on the finite difference method. The calculated pK_a-value of a protonatable site consists of two contributions: the intrinsic p$K_{a,int}$ and the interaction with all other titratable residues in the protein. The p$K_{a,int}$ can further be divided in to three contributions: a) the Born energy p$K_{a,born}$, corresponding to the loss of desolvation energy upon transferring the site from the high dielectric medium (water) to the low dielectric protein environment; b) p$K_{a,back}$, the interaction energy corresponding to interaction of the site with all other protein background charges; and c) the reference p$K_{a,ref}$ of the site in water. The p$K_{a,int}$ together with the interaction energies can be used to calculate the titration behavior of the site. This can be achieved by Monte Carlo (MC) sampling of the 2^N different protonation state of the protein with *N* titrable residues. The KARLSBERG program [39] was used for the MC sampling. The following

reference pK_a-values were used for amino acids: Arg 12.0; Asp 4.5; Glu 4.6; His 6.2; Lys 10.4; Tyr 9.7; heme propionates 4.8. The finite difference grid resolution was 0.25 Å at the region of interest. The membrane region was modeled as a low dielectric slab with $\varepsilon = 4$, protein region as $\varepsilon = 4$ and water filled cavities were described with $\varepsilon = 80$.

3. Results and discussion

MD simulations of fully oxidized *Cc*O (ox/ox, see Section 2.1) suggest that the propionate region of heme a_3 undergoes only very small structural fluctuations from the parent X-ray structure (Fig. 2A). For example, the tight ion pair between the D-propionate of heme a_3 and Arg-438 remains intact, and the A-propionate of heme a_3 remains hydrogen-bonded to Asp-364 and His-368. However, when an electron is inserted in heme *a*, simulating electron transfer from Cu_A, transient and reversible fluctuations are observed, which include conformational changes around the propionates. Thus, Arg-438 dissociates reversibly from the D-propionate of heme a_3 in accordance with previous studies [15,17,18], and structural changes around the A-propionate are observed, as shown in Fig. 2B, C, D: The carboxylate moiety of the A-propionate rotates by ~90° around the C_β–C_γ (CBA–CGA) axis of the side-chain, breaking the hydrogen bond from Asp-364. This new state is referred to here as the "open" conformation in which the hydrogen bonding pattern moreover indicates that there might be direct proton connectivity from Glu-242, via the D-propionate of heme a_3 to the twisted carboxylate of the A-propionate (Fig. 2D). In such a scenario, all oxygen atoms in the proton transfer chain are within hydrogen-bonding distances from one another (~2.5–3 Å). In contrast, in simulations of other redox states (Fig. 2A, C), the hydrogen bond between the A-propionate and Asp-364 remains intact, i.e. in the "closed" conformation, as in the original crystal structure.

Continuum electrostatic calculations give insight in the pK_a values of titratable groups [37]. However, in difficult cases such calculations might suffer from large errors because the pK_a strongly depends on environmental factors, such as the protonation state of all other titratable groups in the protein and errors in classical parameterization. The absolute magnitude of computed pK_a values should therefore be taken with caution, whereas relative pK_a shifts can be considered more reliable. According to our calculations, the pK_a of the A-propionate has an undefined value in the "closed" conformation, indicating that it remains deprotonated within the computed pH range, −15 to 30, irrespective of the oxidation state of the heme *a*. The average pK_a increases strongly in the "open" conformation, reaching a

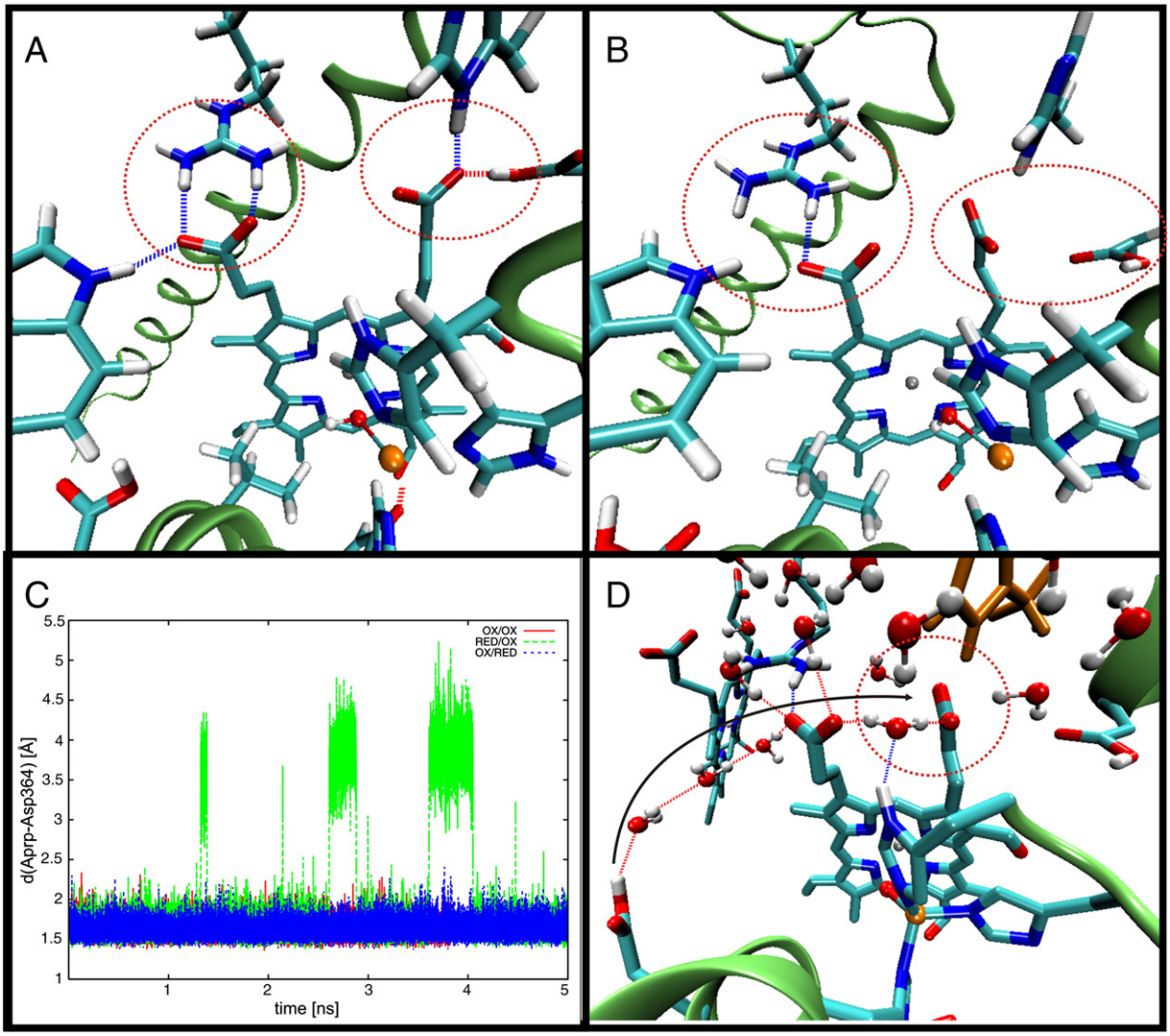

Fig. 2. Transient structure obtained from MD simulation of A) ox/ox, and B) red/ox. C) The distance between the A-propionate of heme a_3 and Asp-364 as a function of simulation time in three different redox-states: ox/ox (red lines), red/ox (green lines), and ox/red (blue lines). Water molecules were omitted from A and B for clarity. D) Snapshot obtained from the red/ox MD simulations illustrating the hydrogen bonded connectivity from Glu-242 to the A-propionate. Subfigures A, B, and D were prepared using VMD [44].

value of ~9.2 ± 3 pK-units when heme *a* is reduced. The average pK_a of the A-propionate for the respective "open" ensemble of structures obtained from the red/ox simulation is ~7.2 ± 3 when C*c*O is fully oxidized. Although the variation of the pK_a within the ensemble of "open" structures is relatively large, for a given structure the pK_a is raised by 2.0 ± 1 pK-units by reduction of heme *a*. The pK_a of the A-propionate in the "open" state with heme *a* reduced is in accordance with independent estimates by Wikström and Verkhovsky [7] and Kaila et al. [28]. The electrostatic calculations also indicate an increase in total protonation probability of the two subunit enzyme upon heme *a* reduction, in accordance with previous studies [19,26]. The partial dissociation of the Arg-438/D-propionate ion pair upon reduction of heme *a* does not increase the pK_a of the D-propionate to a defined value, suggesting that only the A-propionate could act as a pump site, whereas the D-propionate might act as a transient proton transfer site (Fig. 2D). The trajectories obtained from the MD simulations show that the D-propionate/Arg-438 ion pair is always dissociated in the "open" state together with dissociation of the A-propionate/Asp-364 pair, suggesting that there might be a correlation between the two events (Fig. 3). However, the reverse is not the case, i.e. the D-propionate/Arg-438 pair dissociates with higher frequency. Asp-364 is always protonated independently of red/ox state or "closed" vs. "open" conformation, further corroborating the idea that the A-propionate is the protonatable site in this region. Due to the high homology of the area surrounding the PLS among different heme-copper oxidases a similar behavior may be expected, for example in the cbb_3-type oxidases, although homology models suggest that an asparagine replaces the hydrogen bonding aspartic acid [40–42].

Our results suggest that the "open" state of the A-propionate is stabilized statically by at least 2 pK-units on the average (~2.8 kcal/mol at 310 K) by electrostatic polarization when heme *a* is reduced, relative to the fully oxidized state. The equilibrium MD simulations suggest that when heme *a* is reduced the "opening" of the A-propionate interactions has a lower bound transition energy of 1.2 kcal/mol ($G(p) = -\mathrm{RTlog}[p]$ at 310 K, where $p(\mathrm{open}) = 0.15$). When heme *a* is oxidized the best estimate of the forward rate of "opening" is less than 1/(5 ns), which corresponds to a barrier higher than 6.4 kcal/mol ($k = k_0 \exp[-\Delta G^*/\mathrm{RT}]$, $k_0 \sim 6.4\ (\mathrm{ps})^{-1}$). Hence the "opening" is dynamically stabilized by reduction of heme *a* by at least 5.2 kcal/mol (= 6.4–1.2 kcal/mol). It is noteworthy that although six reversible opening transitions are observed when heme *a* is reduced, the free energy estimate given above is approximate. Furthermore, the estimate of the "opening" rate when heme *a* is oxidized is only indicative of the forward barrier height, and rigorous free energy simulations are needed to define the redox-state dependent free energy differences more accurately. Taken together with the static polarization, an approximate overall stabilization of ≥8 kcal/mol (5.2 + 2.8 kcal/mol) is obtained. Based on thermodynamic modeling of the proton-pumping step in C*c*O we found previously that a barrier of ~10.6 kcal/mol is required to effectively prevent proton back-leakage reactions at a membrane potential of 200 mV [28], which is not very far from our approximate lower bound estimate. This barrier may be reached due to lack of an electron at heme *a* in the state where the electron and a proton has been transferred to the BNC and the PLS is loaded. The proton in the PLS is to be ejected to the P-side of the membrane, and the barrier should prevent its back transfer to Glu-242. Our estimate includes the exergonicity of the down-flip of the anionic Glu-242 ([28] cf. also [43]). Siegbahn and Blomberg [29], who did not include the dynamics of the Glu-242 side chain, concluded that the transition state for proton transfer between Glu-242 and the PLS must have an overall positive charge in order to create a barrier sufficiently high to prevent the back-leakage. However, the calculations presented here suggest that static and dynamic polarization of the A-propionate together with the previously suggested Glu-242 valve mechanism might be sufficient to satisfy the requirement for preventing proton leaks. This interpretation is also in agreement with the master equation simulations by Kim et al. [30,31], according to which a redox-controlled proton-loading site ("pump site") is essential for efficient proton pumping. These simulations showed that both the pK_a of the PLS and the proton transfer barrier between Glu-242 and the PLS were modulated by the redox state of heme *a*. Future free-energy simulations are currently in progress to elaborate this question more quantitatively.

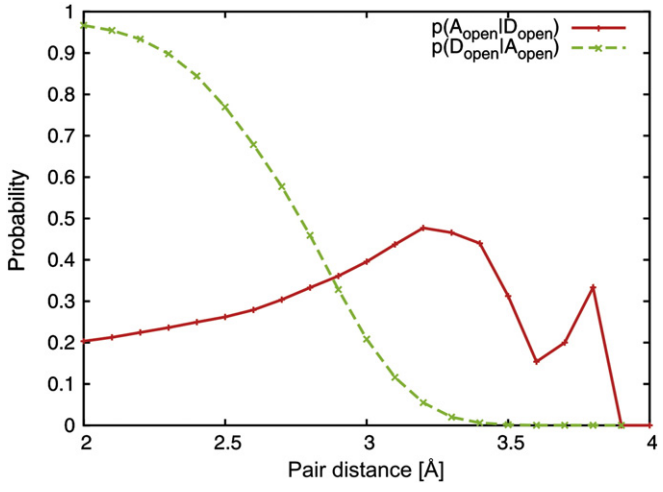

Fig. 3. Correlated opening of the D-propionate (O1D)/Arg-438 (HH22) (D_{open}) and A-propionate (O1A)/Asp-364 (HD2) (A_{open}) ion pairs. The correlation was computed as the conditional probability to observe the A-propionate in an "open" state, given that the D-propionate pair was also "open", $p(A_{open}|D_{open})$, as a function of the pair distance threshold used to define the "open" state, and vice versa for the D-propionate, $p(D_{open}|A_{open})$. The conditional probabilities approach zero as the probability of sampling long pair distances gets lower. The figure shows that it is more probable to observe the A-propionate in an "open" state, when the D-propionate is "open", rather than vice versa. It may therefore be suggested that the latter induces opening of the former.

4. Conclusions

The intimate coupling between electron and proton transfer in C*c*O is of key importance in efficient proton-pumping and safe oxygen reduction. As shown here, reduction of heme *a* causes reversible dissociation of the hydrogen bond to the A-propionate of heme a_3, which increases its pK_a and enables proton transfer from Glu-242. Protonation of the subsequently reduced binuclear site neutralizes the electron charge, which leads to ejection of the proton at the pump site to the P-side of the membrane. By polarizing the pump-site both statically and dynamically the redox state of heme *a* also controls the barrier for proton back leakage. Together with the previously suggested Glu-242 valve it thus helps in releasing the proton to the P-side of the membrane.

Acknowledgement

The work was supported by Biocentrum Helsinki, the Academy of Finland and the Sigrid Jusélius Foundation. V.S. is supported from Viikki Graduate School in Molecular Biosciences. CSC—The Finnish Center for Scientific Computing is acknowledged for computing resources.

References

[1] M.K.F. Wikström, Proton pump coupled to cytochrome *c* oxidase in mitochondria, Nature 266 (1977) 271–273.
[2] S. Ferguson-Miller, G.T. Babcock, Heme copper terminal oxidases, Chem. Rev. 96 (1996) 2889–2908.
[3] G.T. Babcock, M. Wikström, Oxygen activation and the conservation of energy in cell respiration, Nature 356 (1992) 301–309.
[4] M. Yoshida, E. Muneyuki, T. Hisabori, ATP synthase—a marvelous rotary engine of the cell, Nat. Rev. Mol. Cell Biol. 2 (2001) 669–677.
[5] P. Mitchell, Coupling of phosphorylation to electron and hydrogen transfer by a chemi-osmotic type of mechanism, Nature 191 (1961) 144–148.

[6] I. Belevich, D.A. Bloch, N. Belevich, M. Wikström, M.I. Verkhovsky, Exploring the proton pump mechanism in real time, Proc. Natl Acad. Sci. USA 104 (2007) 2685–2690.
[7] M. Wikström, M.I. Verkhovsky, Mechanism and energetics of proton translocation by the respiratory heme-copper oxidases, Biochim. Biophys. Acta 1767 (2007) 1200–1214.
[8] A.A. Konstantinov, S. Siletsky, D. Mitchell, A. Kaulen, R.B. Gennis, The roles of two proton input channels in cytochrome *c* oxidase from *Rhodobacter sphaeroides* probed by the effects of site-directed mutations on time-resolved electrogenic intraprotein proton transfer, Proc. Natl Acad. Sci. USA 94 (1997) 9085–9090.
[9] R.B. Gennis, Coupled proton and electron transfer reactions in cytochrome oxidase, Front. Biosci. 9 (2004) 581–591.
[10] P. Brzezinski, Redox-driven membrane-bound proton pumps, Trends Biochem. Sci. 29 (2004) 380–387.
[11] D. Bloch, I. Belevich, A. Jasaitis, C. Ribacka, A. Puustinen, M.I. Verkhovsky, M. Wikström, The catalytic cycle of cytochrome *c* oxidase is not the sum of its two halves, Proc. Natl Acad. Sci. USA 101 (2004) 529–533.
[12] P.E.M. Siegbahn, M.R.A. Blomberg, Energy diagrams and mechanism for proton pumping in cytochrome *c* oxidase, Biochim. Biophys. Acta 1767 (2007) 1143–1156.
[13] R. Sugitani, E.S. Medvedev, A.A. Stuchebrukhov, Theoretical and computational analysis of the membrane potential generated by cytochrome *c* oxidase upon single electron injection into the enzyme, Biochim. Biophys. Acta 1777 (2008) 1129–1139.
[14] V.R.I. Kaila, M.I. Verkhovsky, G. Hummer, M. Wikström, Glutamic acid 242 is a valve in the proton pump of cytochrome *c* oxidase, Proc. Natl Acad. Sci. USA 105 (2008) 6255–6259.
[15] M. Wikström, C. Ribacka, M. Molin, L. Laakkonen, M.I. Verkhovsky, A. Puustinen, Gating of proton and water transfer in the respiratory enzyme cytochrome *c* oxidase, Proc. Natl Acad. Sci. USA 102 (2005) 10478–10481.
[16] P.E.M. Siegbahn, M.R.A. Blomberg, M.L. Blomberg, A theoretical study of the energetics of proton pumping and oxygen reduction in cytochrome oxidase, J. Phys. Chem. B 107 (2003) 10946–10955.
[17] J. Xu, G.A. Voth, Redox-coupled proton pumping in cytochrome *c* oxidase: further insights from computer simulation, Biochim. Biophys. Acta 1777 (2008) 196–201.
[18] A.V. Pisliakov, P.K. Sharma, Z.T. Chu, M. Haranczyk, A. Warshel, Electrostatic basis for the unidirectionality of the primary proton transfer in cytochrome *c* oxidase, Proc. Natl Acad. Sci. USA 105 (2008) 7726–7731.
[19] A. Kannt, C.R. Lancaster, H. Michel, The coupling of electron transfer and proton translocation: electrostatic calculations on *Paracoccus denitrificans* cytochrome *c* oxidase, Biophys. J. 74 (1998) 708–721.
[20] D.M. Popovic, A.A. Stuchebrukhov, Proton pumping mechanism and catalytic cycle of cytochrome *c* oxidase: Coulomb pump model with kinetic gating, FEBS Lett. 566 (2004) 126–130.
[21] D.M. Popovic, J. Quenneville, A.A. Stuchebrukhov, DFT/electrostatic calculations of pK_a values in cytochrome *c* oxidase, J. Phys. Chem. B 109 (2005) 3616–3626.
[22] J. Quenneville, D.M. Popovic, A.A. Stuchebrukhov, Redox-dependent pK_a of Cu_B histidine ligand in cytochrome *c* oxidase, J. Phys. Chem. B 108 (2004) 18383–18389.
[23] E. Fadda, N. Chakrabarti, R. Pomès, Acidity of a Cu-bound histidine in the binuclear center of cytochrome *c* oxidase, J. Phys. Chem. B 109 (2005) 22629–22640.
[24] E. Fadda, C.H. Yu, R. Pomès, Electrostatic control of proton pumping in cytochrome *c* oxidase, Biochim. Biophys. Acta 1777 (2008) 277–284.
[25] Y. Song, J. Mao, M.R. Gunner, Electrostatic environment of hemes in proteins: pK_as of hydroxyl ligands, Biochemistry 45 (2006) 7949–7958.
[26] Y. Song, E. Michonova-Alexova, M.R. Gunner, Calculated proton uptake on anaerobic reduction of cytochrome *c* oxidase: is the reaction electroneutral? Biochemistry 45 (2006) 7959–7975.
[27] H.J. Lee, L. Ojemyr, A. Vakkasoglu, P. Brzezinski, R.B. Gennis, Properties of Arg481 mutants of the aa_3-type cytochrome *c* oxidase from *Rhodobacter sphaeroides* suggest that neither R481 nor the nearby D-propionate of heme a_3 is likely to be the proton loading site of the proton pump, Biochemistry 48 (2009) 7123–7131.
[28] V.R.I. Kaila, M.I. Verkhovsky, G. Hummer, M. Wikström, Mechanism and energetics by which glutamic acid 242 prevent leaks in cytochrome *c* oxidase, Biochim. Biophys. Acta 1787 (2009) 1205–1214.
[29] P.E.M. Siegbahn, M.R.A. Blomberg, Proton pumping mechanism in cytochrome *c* oxidase, J. Phys. Chem. 112 (2008) 12772–12780.
[30] Y.C. Kim, M. Wikström, G. Hummer, Kinetic models of redox-coupled proton pumping, Proc. Natl Acad. Sci. USA 104 (2007) 2169–2174.
[31] Y.C. Kim, M. Wikström, G. Hummer, Kinetic gating of the proton pump in cytochrome *c* oxidase, Proc. Natl Acad. Sci. USA 106 (2009) 13707–13712.
[32] T. Tsukihara, K. Shimokata, Y. Katayama, H. Shimada, K. Muramoto, H. Aoyama, M. Mochizuki, K. Shinzawa-Itoh, E. Yamashita, M. Yao, Y. Ishimura, S. Yoshikawa, The low-spin heme of cytochrome *c* oxidase as the driving element of the proton-pumping process, Proc. Natl Acad. Sci. USA 100 (2003) 15304–15309.
[33] A.D. MacKerell Jr., D. Bashford, M. Bellott, R.L. Dunbrack Jr., J.D. Evanseck, M.J. Field, S. Fischer, J. Gao, H. Guo, S. Ha, et al., All-atom empirical potential for molecular modeling and dynamics studies of proteins, J. Phys. Chem. B 102 (1998) 3586–3616.
[34] M.P. Johansson, V.R.I. Kaila, L. Laakkonen, Charge parameterization of the metal centers in cytochrome *c* oxidase, J. Comp. Chem. 29 (2007) 753–767.
[35] S. Riistama, G. Hummer, A. Puustinen, R.B. Dyer, W.H. Woodruff, M. Wikström, Bound water in the proton translocation mechanism of the haem-copper oxidases, FEBS Lett. 414 (1997) 275–280.
[36] J.C. Phillips, R. Braun, W. Wang, J. Gumbart, E. Tajkhorshid, E. Villa, C. Chipot, R.D. Skeel, L. Kale, K. Schulten, Scalable molecular dynamics with NAMD, J. Comp. Chem. 26 (2005) 1781–1802.
[37] D. Bashford, K. Gerwert, Electrostatic calculations of the pk_a values of ionizable groups in Bacteriorhodopsin, J. Mol. Biol. 224 (1992) 473–486.
[38] D. Bashford, An object-oriented programming suite for electrostatic effects in biological molecules, in: Y. Ishikawa, R.R. Oldenhoeft, J.V.W. Reynders, M. Tholburn (Eds.), Scientific Computing in Object-Oriented Parallel Environments, Springer, Berlin/Heidelberg, 1997, pp. 233–240.
[39] B. Rabenstein, E.W. Knapp, Calculated pH-dependent population and protonation of carbon-monoxy-myoglobin conformers, Biophys. J. 80 (2001) 1141–1150.
[40] V. Sharma, A. Puustinen, M. Wikström, L. Laakkonen, Sequence analysis of the cbb_3 oxidases and an atomic model for the *Rhodobacter sphaeroides* enzyme, Biochemistry 45 (2006) 5754–5765.
[41] V. Sharma, M. Wikström, L. Laakkonen, Modeling the active-site structure of the cbb_3-type oxidase from *Rhodobacter sphaeroides*, Biochemistry 47 (2008) 4221–4227.
[42] J. Hemp, D.E. Robinson, K.B. Ganesan, T.J. Martinez, N.L. Kelleher, R.B. Gennis, Evolutionary migration of a post-translationally modified active-site residue in the proton-pumping heme-copper oxygen reductase, Biochemistry 45 (2006) 15405–15410.
[43] N. Ghosh, P.R. Xavier, M.R. Gunner, Q. Cui, Microscopic pK_a analysis of Glu286 in cytochrome *c* oxidase (*Rhodobacter sphaeroides*): toward a calibrated molecular model, Biochemistry 48 (2009) 2468–2485.
[44] W. Humphrey, A. Dalke, K. Schulten, VMD—visual molecular dynamics, J. Mol. Graph. 14 (1996) 33–38.